VOLUME - 11, ISSUE - 12, DECEMBER - 2022 • PRINT ISSN No. 2277 - 8160 • DOI : 10.36106/gjra

Original Research Paper

Radio-Diagnosis

# CT AND MRI EVALUATION OF EXTENT, PATHWAYS OF SPREAD AND POST-OPERATIVE FINDINGS IN COVID-19 ASSOCIATED RHINO-ORBITAL-CEREBRAL MUCORMYCOSIS

| | |
|---|---|
| **Dr. Manisha V. Joshi** | M.D., DNB, Fellowship in diagnostic Neuroradiology, Assistant Professor, Department of Radiology, BYL Nair Hospital, |
| **Dr. Seshasai Mopuri*** | M.D. Radiology, Senior resident, Department of Radiology, BYL Nair Hospital *Corresponding Author |
| **Dr. Vipul Chemburkar** | D.M.R.E, M.D. Radiology, DNB, Associate Professor, Department of Radiology, BYL Nair Hospital |
| **Dr. Dev Shetty** | M.D. Radiology, Professor and Head of Department, Department of Radiology, BYL Nair Hospital |

## ABSTRACT

**Background:** Recent surge in the number of COVID-19 associated mucormycosis highlights the importance of understanding CT and MRI findings for evaluation of the disease with high morbidity and mortality despite treatment. **Objective:** The purpose of the study is to evaluate CT and MRI imaging findings in patients with Rhino-orbital-cerebral mucormycosis (ROCM) associated with COVID-19 and to highlight the role of MRI and CT in evaluation of extent of ROCM. **Methods:** Retrospective evaluation of MRI and CT findings of 120 patients with proven mucormycosis on potassium hydroxide mount and history of COVID-19 disease within past month was carried out. CT and MRI imaging findings were reviewed for extent of ROCM in paranasal sinuses, orbits, and brain on 64 slice multidetector CT and 1.5 T MRI machine. **Results:** Diabetes (75.8%) and steroid treatment (64.1%) were commonly associated with invasive ROCM in patients with COVID-19. On CT and MRI imaging, 45.8% patients showed involvement of orbits, 41.6% had extension in soft tissue including pre-maxillary, retro-antral region, 40.8% exhibited extension into pterygopalatine fossa and 34.1% showed intracranial extension. Orbital extension presented as abnormal soft tissue in extra-conal (65.4%, 36 of 55) and intraconal compartments followed by optic neuritis. The most preferred route of spread to orbits was from ethmoidal sinuses through direct invasion of lamina papyracea. Intracranial extension most commonly exhibited as cavernous sinus thrombophlebitis (34.1% 14 of 41), followed by pachymeningitis. Perineural spread was seen in 40% of total patients with optic nerve being commonest. **Conclusion:** Based on our study, peri-neural and vascular spread were equally common pathways of spread of infection as compared to direct spread. Common areas of recurrent infection in patients who underwent FESS were orbit, retro-antral region, pterygo-palatine fossa, pre-maxillary region, intra-cranial and palate. Orbital and pterygo-palatine fossa were most common locations of spread of the infection in conservatively managed patients. Diabetes mellitus and steroid treatment were common co morbidities associated with rhino-orbital-cerebral mucormycosis. MRI is an exemplary modality for evaluation of extension of ROCM as it allows assessment of soft tissues. CT plays complimentary role for evaluation of bony structures.

**KEYWORDS :** Rhino orbital cerebral mucromycosis (ROCM), perineural spread, intracranial extension, COVID-19.

## INTRODUCTION:

India has witnessed an exponential surge in the number of COVID-19 associated mucormycosis [1]. Mucormycosis is an opportunistic fungal infection which was seen mostly in immunocompromised patients. Rhino-Orbital-Cerebral mucormycosis (ROCM) is an uncommon infection having high morbidity and mortality despite treatment. This fungal infection can rapidly progress and lead to severe and irreversible damage in individuals who are immunologically or metabolically compromised such as patients who have developed COVID-19 in the recent past. Contributing and aggravating risk factors include diabetes mellitus, steroid administration, HIV infection and immunosuppressive drugs [1]. These lead to a state of hyperglycemia and high oxidation potential which are conducive for the growth of the fungi and its spores. Early suspicion, rapid diagnosis, and initiation of treatment are the most important factors that determine prognosis of mucormycosis. Imaging is essentialfor management in patients with ROCM. CT and MRI imaging studies rapidly provide corroborative evidence when the disease is clinically suspected [1].

In patients with proven ROCM, imaging plays an important role in determining the extent of disease, which is critical in deciding on the further line of management. It is thus imperative for every member of the multidisciplinary team involved in managing these patients to be familiar with the interpretation of the computed tomography (CT) and magnetic resonance imaging (MRI) in ROCM. In the current communication, we elaborate on imaging findings which include most affected sites, routes of extension, complications, location of residual/ recurrent lesions after conservative and post-operative management.

## METHODS:

### *Inclusion criteria:*

This retrospective study was carried out from November 2020 to May 2022 at a tertiary care hospital dedicated exclusively to COVID-19 patient care. All patients were evaluated for paranasal sinuses, orbits and brain with and without contrast on a 64 slice multidetector CT (Philips Brilliance) and 1.5 Tesla MRI machine (Philips Achieva) for ROCM.

Total 120 patients with sino-orbital-cerebral symptoms with COVID-19 confirmed by reverse transcriptase-polymerase chain reaction within the past 1 month and invasive ROCM confirmed by using potassium hydroxide mount of nasal discharge or scrapings after FESS, referred for MRI and CT scan were included in the study. The clinical details concerning ROCM, COVID-19 illness and treatment received were recorded through the hospital management information system. All 120 patients had undergone non-enhanced CT and MRI. For 100 out of 120 patients contrast-enhanced (CE) MRI and CE CTwas performed. Rest of the 20 patients had impaired renal function. The institutional ethics committee approval was granted for this retrospective descriptive study along with a waiver of informed consent.

Out of 120 patients 22 patients had undergone Functional endoscopic Sinus Surgery (FESS) and post-operative follow-

up MRI and CT done. Suspicious recurrence on imaging was confirmed on follow-up FESS and KOH mount.

***Techniques:***

**MRI technique:**

MR examination of PNS and nasal cavity was done in supine position with dedicated head coils.

- 3-4 mm thick slices were acquired including top of frontal sinuses superiorly and level of the jaws inferiorly.
- Brain assessment included – Diffusion, FLAIR, T2, T1, DWI images and post-contrast with TOF angiography

**CT technique:**

Contrast-enhanced CT scan of PNS and nasal cavity was performed after intravenous bolus injection of non-ionic iodinated contrast administered at a dose 1-1.25 ml/kg body weight and with 120kVP and 100mA tube current.

- Thin axial scans of 1- 2mm thickness were obtained and evaluated in both soft tissueand bone windows.

***Interpretation of various imaging parameters:***

The sinuses showing air-fluid levels, mucosal thickening and/or necrotic/non-enhancing soft tissue on CT or MRI were recorded in each case. The following imaging parameters were assessed:

**Pterygopalatine fossa (PPF)**

PPF involvement was defined as obliteration or replacement of the fat with abnormal soft tissue, widening of PPF and bony erosion of its walls. Replacement of fat by abnormal soft tissue and perineural spread were evaluated.

**Perineural spread**

On MRI, findings suggestive of perineural spread were diffuse or focal enlargement of nerve, irregularity, excessive enhancement of a cranial nerve or its branches (either within the cisternal portion or within a canal or foramen), formation of perineural abscess, loss of normal fat pad adjacent to foramen, or widening/excessive enhancement.

**Periosteal involvement of orbital walls**

Periosteal involvement was defined as presence of linear hyperintensity on T2W, STIR coronal MRI.

**Intracranial involvement**

Patients with dural enhancement, presence of extradural collections, infarcts, cerebritis and intracerebral abscess and nerve involvement at the level of skull base foramina, venous sinus thrombosis/ thrombophlebitis and arterial thrombosis, arteritis or mycotic aneurysm were included in intracranial extension.

The imaging findings were reviewed by two diagnostic radiologists with 15 and 11 years of experience. The reviewers were blinded to patients' history, clinical details and earlier imaging examinations. In event of discrepancy amongst the two reviewers, opinion of third radiologist with 30 years of experience was taken and considered as final verdict.

**Statistical Analysis:**

Analytic methods for descriptive studies were used for statistical analysis.

**RESULTS:**

***Demographics and History:***

Demographic, Clinical details and details of treatment of COVID-19 are mentioned in **Table 1.**

Table 1 Demographic, Clinical details and details of treatment of COVID-19

| Variable | Value |
|---|---|
| Patients | 120 |
| Sex | Male: 78, female: 42 |
| Age | <25years:15, 25-60 years:71, >60years:34 |
| Comorbidities | |
| Diabetes mellitus | Known: 51 Newly detected:40 Total: 91 (75.8%) |
| Hypertension | 56 (46.6%) |
| Chronic Kidney Disease | 21 (17.5%) |
| Retroviral disease | 19 (15.8%) |
| Chronic liver disease | 8 (6.6%) |
| Asthma | 5 (4.1%) |
| Chronic Obstructive Airway Disease | 4 (3.3%) |
| Thalassemia | 3 (2.5%) |
| Details of COVID-19 illness | |
| RTPCR positive | All |
| Vaccination done | Yes:0,No: 120 |
| Home isolation | 11 (9.1%) |
| Hospitalised | 109 (90.8%) |
| Steroid treatment received in | 77 (64.1%) |
| Remdesivir | 68 (56.7%) |
| Tocilizumab | 39 (3.3%) |
| Serum ferritin raised | 85 (70.8%) |
| FESS | 22 (18.3%) |
| Surgical Debridement | 7 (5.8%) |

Males in age group of 25-60 years were most commonly affected. Diabetes mellitus (n=91, 75.8%) was the predominant co morbidity associated with ROCM (Known: 51, Newly detected:40) in our study and steroid treatment was given to 77 (64.1%) patients during COVID-19 illness who were later detected with ROCM. 68 patients had received Remdesivir and 39 patients had received Tocilizumab.

All the patients had received intravenous Amphotericin B, 85(70.8%) were conservatively managed, 22 (18.3%) underwent FESS, 7 (5.8%) had open surgical debridement done. Overall mortality in this study was 25(20.8%).

***Sino- nasal disease:***

The disease involved paranasal sinuses (PNS) in all 120 patients and the nasal cavity was involved in 55(45.8 %) patients.

Paranasal sinuses (PNS), nasal cavity, extra-sinus soft tissue and pterygopalatine fossa were evaluated for various parameters as mentioned in **Table 2**.

Table 2 Imaging parameters for paranasal sinuses (PNS), nasal cavity, extra-sinus soft tissue and pterygopalatine fossa:

| parameter | Number of cases |
|---|---|
| 1)Nasal Cavity | 55 |
| • Turbinates (black turbinate) | 10 |
| • Septum | 8 |
| • Meatus | 5 |
| • Drainage pathway OMU/FSDP/SER* | 26/11/18 respectively |
| 2)Paranasal sinuses | 120 |
| • Mucosal edema | 120 (100%) |
| • Mucosal and luminal T2 hypointensity | 67 |
| • Restricted diffusion in mucosa | 40 |
| • Non-enhancing necrotic tissue | 49/100 |
| 3)Extra sinus Soft tissue involvement | 50 |
| • Preantral | 9 |
| • Retro-antral | 41 |
| 4)Pterygopalatine fossa involvement | 59 |
| • sphenopalatine foramen | 7 |
| • pterygomaxillary fissure | 33 |
| • infratemporal fossa involvement | 19 |

Key- OMU- osteo-meatal unit, FSDP- frontal sinus drainage pathway.

On CT, 115(95.8%) patients had maxillary sinus involvement. A total of 60 (50%), 28 (23.3%), and 33(27.5%) patients exhibited involvement of the ethmoid air cells, sphenoidal sinus, and frontal sinuses, respectively. Unilateral involvement was predominant. On CT scan,104 (86.6%) patients exhibited bony erosions of the walls of the PNS. Few of these patients also showed bony erosions of hard palate, superior alveolar ridge and bony nasal septum. Bony erosions and permeative lytic destruction on CT were associated with mottled air density foci and non-enhancing osseous necrosis within the involved bones on contrast enhanced T1W fat-saturated images **(Figure 1 a, b).**

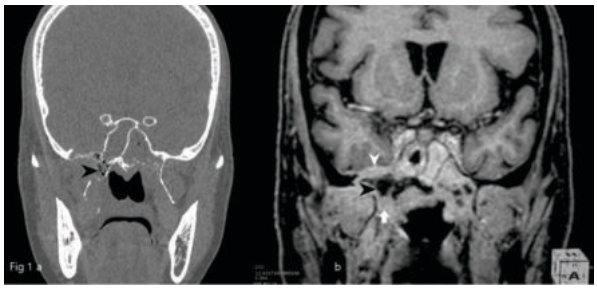

**Fig. 1a.** 37-year-old male with mucormycosis involving sphenoid bone. CT coronal image of mottled air density foci in right greater wing of sphenoid and root of pterygoid plates (black arrowhead).

**Fig 1b.** MRI T1 contrast enhanced coronal image of same patient shows non enhancing ischemic bone necrosis in the corresponding areas (black arrowhead). Linear homogenous enhancement and thickening of dura noted in right middle cranial fossa (white arrowhead). Right PPF and infra temporal fossa are involved in the form of abnormal soft tissue showing subtle enhancement (white arrow).

Surrounding walls of involved sinuses were normal in 16 cases (13.3 %) with spread of infection across uninvolved bone into the peri-sinus fat. Hard palate erosions were seen in 15 (12.5%) patients, 4 of them exhibited oro-nasal fistula and 3 showed oro-antral fistula. 27 (22.5%) patients showed hyperdense sinus content. On contrast enhanced MRI images, 51 patients showed enhancing mucosa and soft tissue and 49 patients showed patchy areas of lack of enhancement within the soft tissue and mucosa representing ischemic necrosis.10 patients exhibited focal areas of lack of mucosal enhancement in turbinates. 40 (33.3%) of these patients also exhibited mucosal restricted diffusion and drop in signal on corresponding ADC image. Septal perforation was seen in 4 patients with nasal cavity whilst osteomeatal unit (OMU), frontal sinus drainage pathway (FSDP) and spheno-ethmoid recess (SER) were obliterated in 26,11 and 18 patients respectively.

The retro-antral soft tissue rind was exhibited by 41(34%) patients which was best delineated on T2W and fat-suppressed post contrast T1W images, as edema and enhancement respectively. Further extension in infra-temporal fossa was seen as edema and enhancement within the muscles of mastication in 19 (15.8%) patients.

***Orbital disease extension:***

Total 55(45.8%) patients showed extension in orbits as depicted in **Table 3**.

| Table 3 Imaging parameters for orbital involvement (55 patients) | |
|---|---|
| periosteum | 21 |
| Intraconal fat | 24 |
| extraconal fat | 36 |
| extraocular muscles | 10 |
| globe | 2 |
| Optic nerve | 21 |
| orbital apex | 24 |
| SOF* | 24 |
| IOF** | 13 |
| Ethmoidal vein thrombosis | 4 |
| SOV ^ thrombosis | 2 |
| Perivascular spread along ophthalmic artery | 1 |
| Imaging parameters for intracranial involvement (41 patients) | |
| Cavernous sinus thrombophlebitis | 14 (34.1%) |
| ICA* thrombosis | 4 (9.7%) |
| Mycotic aneurysm | 2 (4.8%) |
| Meckel's cave | 7 (17%) |
| Pachymeningitis | 13 (31.7%) |
| Brain parenchyma: Infarct | 5 (12.1%) |
| Cerebritis | 4 (9.7%) |
| Abscess | 4(9.7%) |

| Imaging of perineural spread (48) | | | |
|---|---|---|---|
| Nerve | Enhancement with or without thickening | Restricted diffusion in thickened or non-thickened nerves. | Abscess formation |
| Optic nerve | 11 | 4 | 2 |
| V1 (SOF) | 3 | 3 | 1 |
| V2 (IOF) | 8 | 5 | 2 |
| V3(F. Ovale) | 6 | 2 | 2 |
| Trigeminal nerve cisternal segment and Meckel's cave | 5 | 1 | 1 |
| Vidian nerve | 1 | 5 | 0 |
| Infra-orbital nerve | 12 | 10 | 0 |
| Greater palatine nerve | 1 | 1 | 0 |

Key- SER- spheno-ethmoidal recess, *SOF- superior orbital fissure, **IOF- inferior orbital fissure, ^SOV- superior ophthalmic vein, *ICA- internal carotid artery.

The spread of the disease into orbits was seen predominantly through direct tissue invasion and hence extraconal fat involvement was seen in more patients (36, 65% in patients with orbital involvement) than those with intraconal fat involvement (24, 43.6%).

Out of 60 patients who exhibited involvement of ethmoid air cells, 38 patients showed involvement of medial orbits with erosions and attenuation of lamina papyracea seen in 32 patients.

The most preferred route of spread to orbits wasdirect tissue invasion from ethmoidal sinuses through lamina papyracea and from maxillary sinuses through inferior wall of orbits.

Another pathway for spread of disease was found through natural bony ostia for anterior and posterior ethmoidal arteries. 6 such patients typically exhibited soft tissue in superior-nasal extraconal fat **(Figure 2 a, b)** without erosions of lamina papyracea.

One of the patients also showed extension of soft tissue further along the course of ophthalmic artery in intraconal compartment.

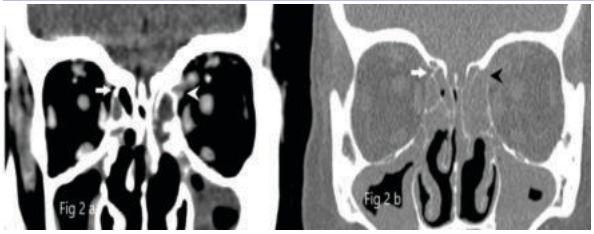


**Fig. 2a**. 56-year-old male with retro-orbital pain after FESS and debridement. Soft tissue window CT coronal image on showing extension of the infection from left ethmoidal foramen with replacement of foraminal fat by abnormal soft tissue (white arrowhead). Normal right ethmoid foramen is demonstrated by with preserved fat density within (white arrows).

**Fig. 2b**. Bone window CT coronal image of same patient showing widening of the left ethmoid foramen (black arrowhead). Normal right ethmoid foramen is demonstrated by with preserved fat density within (white arrows).

Optic nerve involvement was seen in 21 patients. Perineural enhancement and altered nerve signal intensity was the most common finding and was seen in 14 patients. Restricted diffusion was seen in optic nerves in 5 patients.

Formation of fungal abscess was seen in 2 patients in the form of perineural collection, one of the patients also exhibited hemorrhage within the perineural abscess **(Figure 3a, b)**.

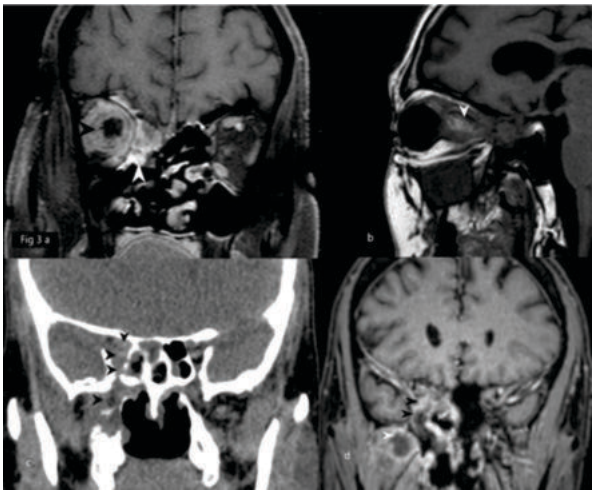


**Fig. 3a**- 41-year-old female who is a known case of HIV and mucormycosis. T1 post contrast coronal image showing non-enhancing area surrounded by abnormally enhancing soft tissue suggestive of abscess in the right orbit (black arrowhead) and heterogeneously enhancing soft tissue in the right ethmoid sinuses (white arrowhead).

**Fig. 3b**- T1 oblique sagittal image of the right orbit in the same patient showing hyperintense areas within the abscess suggestive of haemorrhage (white arrowhead).

**Fig. 3c**- 60-year-old male with recurrence of mucormycosis post-FESS. CT coronal image showing replacement of fat by abnormal soft tissue in right orbital apex including superior orbital fissure, inferior orbital fissure and pterygo-palatine fossa (black arrowheads) from above downwards.

**Fig. 3d**- T1 post-contrast coronal image in same patient showing replacement of fat by abnormal enhancing soft tissue in right orbital apex (black arrowheads) with a peripherally enhancing abscess like collection in right pterygopalatine fossa and infratemporal fossa (white arrowhead).

Enhancing soft tissue at the orbital apex extending into superior orbital fissure and optic canal was seen in 24 (20%) patients representing orbital apex syndrome **(Figure 3 c, d).**

***Intracranial disease extension:***

Out of 120 patients, 41 (34.1%) patients exhibited intracranial spread as mentioned in **Table 3**.

We discovered that intracranial extension was seen through various pathways. Direct spread was seen most commonly through tissue invasion, i.e., across the cribriform plate, walls of the ethmoid, and frontal sinuses. Other modes of spread were through anatomical apertures, perineural and perivascular spread.

Cavernous sinus thrombophlebitis (n=14, 34.1%) was the commonest imaging finding (Figure 13) amongst the patients with intracranial extension followed by pachymeningitis (n=13,31.7%) in middle and anterior cranial fossa. Early intracranial spread in the form of meningeal enhancement was better appreciated on contrast enhanced T1W images.Brain parenchyma was commonly affected by infarcts secondary to vasculitis (n=5, 12.1%).

Development of a well-delineated mass with liquified central T2 hyperintense core showing diffusion restriction representing abscess formation was seen 4 patients, all involving temporal lobes. T2 hypointense internal papillary projections were also exhibited in one of the cases **(Figure 4 a).**

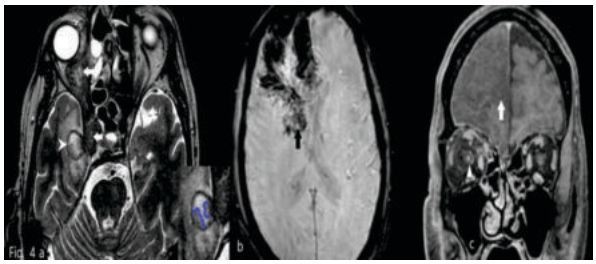


**Fig 4a**. 33-year-old male on steroids for COVID-19. T2 axial image showing hyperintense abscess with T2 hypointense rim in right temporal lobe (arrow head). The intracranial abscess is seen as an extension of the abscess along the right optic nerve and right cavernous sinus (white arrows). Lower right corner showing zoomed in view showing T2 hypointense papillary projections within the abscess.

**Fig. 4b**. 59-year-old male who had mucormycosis and intra-cranial extension in form of cerebritis, axial gradient image shows areas of blooming in right frontal lobe.

**Fig. 4c.** Same patient with cerebritis, on T1 contrast enhanced image, non-enhancing hypointense area in right frontal lobe with parenchymal edema in the form of sulcal space obliteration. Intraorbital extension seen as abnormal intraconal soft tissue on superomedial aspect and optic nerve perineuritis (white pointer).

Few (4, 9.7 %) patients presented with direct intracranial extension in form of cerebritis, seen as ill-defined areas of restricted diffusion and hemorrhages **(Figure 4 b, c)**.

All the 11 cases of cavernous sinus thrombophlebitis also exhibited associated orbital apex syndrome i.e. involvement of optic canal and superior orbital fissure (SOF). Heterogeneously enhancing soft tissue with convexity on the lateral aspect of the cavernous sinus was seen in these patients. There was associated dilatation of superior ophthalmic vein (SOV). SOV thrombosis was seen in two patients in the form of loss of flow void on T2WI and non-opacification of the vein on contrast enhanced MRI.

Middle cranial fossa involvement in the form of pachymeningitis was seen to be associated with pterygopalatine fossa and inferior orbital fissure involvement in 5 patients.

Perivascular spread was seen predominantly involving ICA in the form of vasculitis, thrombosis and mycotic aneurysms **(Figure 5 a, b)** in 4 (9.7 %) and 2 (4.8%) patients respectively.

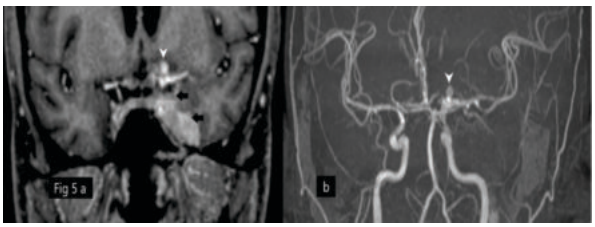


**Fig. 5a**. 74-year-old male with headache. Post-contrast T1 fat saturated coronal image of mycotic aneurysm at origin of left MCA (white arrowhead) with left cavernous sinus thrombophlebitis in the form of abnormally enhancing soft tissue and convexity of lateral margin (black arrows).

**Fig. 5b**. TOF angiogram coronal image of same patient depicting mycotic aneurysm (white arrowhead) at origin of MCA.

***Perineural spread (PS)***

Total 48 (40% of total) patients showed perineural spread (PS).Optic nerve (17, 35.4 %). was the commonest nerve involved followed by maxillary division of trigeminal nerve (15, 31.2%).

Perineural spread was presented in three different forms as mentioned in **Table 3**.

I) Enhancement with or without thickening of nerves.
ii) Restricted diffusion on DWI sequence **(Figure 6b)** in thickened or non-thickened nerves.
iii) Perineural abscess formation.

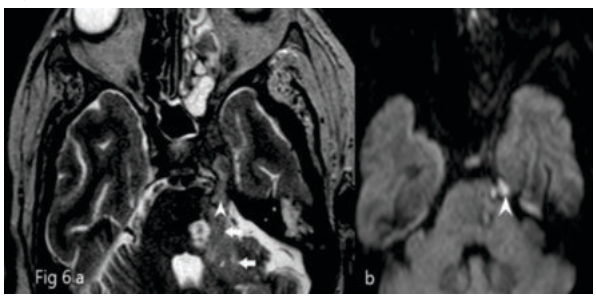


**Fig. 6a**. 49-year-old female with uncontrolled diabetes. Perineural spread along the cisternal portion of left trigeminal nerve with a T2 hyperintense abscess showing distinct hypointense rim (white arrowhead) and chronic infarcts of left hemipons, middle cerebellar peduncle and cerebellum (white arrowheads). Loss of flow void with wall thickening in cavernous segment of left ICA (black arrowhead)

**Fig. 6b**. Restricted diffusion on DWI in same patient in cisternal part of left trigeminal nerve (white arrowhead).

Perineural spread from the cavernous sinus, along the trigeminal nerve, had led to posterior fossa involvement in 7 patients **(Figure 6a)**.

Optic nerve was overall the commonest nerve involved and most of these patients had presented with vision loss/ diminished vision.

Maxillary division of trigeminal nerve (V2) was the most common division involved secondary to involvement of PPF, IOF and foramen rotundum.

The mandibular division of trigeminal nerve (V3) was involved in 10 (8.3%) patients and 2 of them exhibited perineural abscess formation. Effacement of CSF space of Meckel's cave was seen in 7 (17 %) patients with intracranial spread of infection along trigeminal nerve.

Most of these patients with PS had also exhibited involvement of the PPF as it represents the crossroads of various neural foramina. The pterygopalatine fossa was involved in 49 out of 120 (40.8%) patients **(Figure 7 a, b)**.

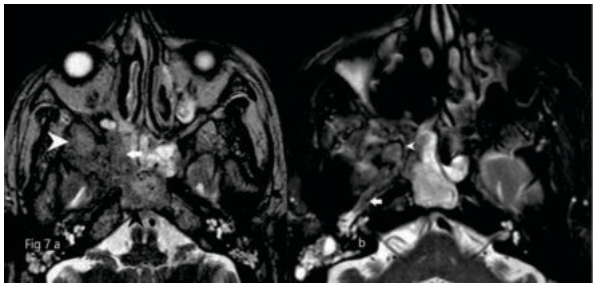


**Fig. 7a**. 66-year-old male with HIV, Diabetes, hypertension and on steroids for COVID-19. T2 axial image depicting extension of mucormycosis into right pterygopalatine fossa from right sphenopalatine foramen (white arrow) with extension into infra-temporal (large white arrowhead) and clivus (black arrowhead).

**Fig. 7b**. 50-year-old male with history of mucormycosis post-FESS. Axial T2 SPIR image showing involvement of the infection into right pterygopalatine fossa (small white arrowhead) with extension into right Eustachian tube causing right otomastoiditis (white arrow).

## DISCUSSION:

In the pre-COVID-19 era, the incidence rate of mucormycosis varied from 0.005 to 1.7 per million on a worldwide scale [2]. Whereas, in India, its prevalence was 0.14 per 1000, which compared to developed countries was 80 times higher. The outbreak of COVID -19 in India was followed by a huge surge of secondary infection of ROCM.

We described CT and MRI imaging findings of ROCM in 120 post-COVID-19 patients. 75.8% of patients had diabetes mellitus and to a lesser extent, other co-morbidities were seen. Ismaiel WF et al found diabetes mellitus in 44.4% of post-COVID-19 acute invasive fungal rhinosinusitis (AIFRS) [3]. They also found that diabetes mellitus was the leading underlying co-morbidity in AIFRS (50%) and also listed HIV, leukemia, and immune suppression among others. This may be due to the fungal affinity for an acidic environment with disproportionately high glucose concentration as observed by Watkinson JC [4].

The presence of bony erosions of walls of paranasal sinuses with air foci within the involved bone was also seen in the study by Joshi AR et al [5]. In our study, additionally, osseous ischemic necrosis was found on CE T1W fat-saturated images in the involved bony structures. Other complications involving bony erosions included the formation of an oro-antral fistula.

The invasive nature of the disease in the form of peri-antral soft tissue, involvement of PPF and infratemporal fossa, and extra-sinus spread into orbits and intracranial extension was seen in our study. Peri-antral soft-tissue infiltration represented one of the imaging findings suggestive of invasive disease.

In our study, we found that the supero-nasal and medial extraconal fat was the commonest site of involvement in orbit due to direct invasion through lamina papyracea which is the thinnest orbital wall, and the presence of multiple bony Ostia

which provide an easy path for the spread of infection from the ethmoidal sinuses. Similar to Hosseini SM et al we found that orbital invasion in mucormycosis typically occurs through pathways with a lower number of natural barriers, which include lamina papyracea and ethmoid foramina [6].

Our study includes cases with most of the complications of ROCM in paranasal sinuses, nasal cavity, oral cavity, intra-cranial, orbital and extra-sinusoidal spread, by main pathways of infection spread that are direct dissemination, through natural foramina, perineural and perivascular spread similar to Ma J et al [7]. Safder S. et al found that direct invasion of the anterior cranial fossa occurs through erosions of ethmoid bone (cribriform plate), which may or may not be associated with meningitis, encephalitis, or brain abscess formation [8].

PPF is a major site of neurovascular bundle crossings between the oral cavity, nasopharynx, orbit, masticator space, infratemporal fossa, middle cranial fossa, and nasal cavity. Its multitude of complex connections and important location can potentially form an easy conduit for the spread of inflammatory and neoplastic diseases across the various deep spaces in the head and neck.

Our study highlights the importance of perineural spread (PS) and the imaging pattern was divided into 3 categories i.e., enhancement, lack of enhancement associated with or without diffusion restriction, and perineural abscess formation.

In the past, the perineural spread was considered unusual. However, many emerging studies have demonstrated possible PS with histopathology, gross specimens, and radiology studies. Particularly, Sravani et al. proved that perineural spread is possible even at a significant distance away from the primary focus of infection in more than half of the patients suffering from ROCM using biopsy specimens [9]. Other authors have demonstrated perineural spread along large-diameter nerves, also visible on MRI imaging, that is inclusive of the three branches of the trigeminal nerve. Margo et al. described the ophthalmic division of trigeminal nerve involvement in a patient with invasive mucormycosis in the front half of the orbit [10]. The maxillary division of trigeminal nerve involvement retrogradely from the infra-orbital nerve and dissemination to the pterygopalatine fossa passing from the inferior orbital fissure and to the middle cranial fossa via foramen rotundum, was also reported by Parsi K et al [11]. Similar to Orguc S et al we have also reported cavernous sinus, Meckel's cave, and the cisternal segment of trigeminal nerve involvement, with a varied affection of the pons and brainstem [12].

Invasive mucormycosis has a propensity to invade intracranial vessel walls, form septic thrombi, and manifest as acute septic strokes, cavernous sinus thrombosis, mycotic aneurysms, and vessel wall inflammation which were reported by Dusart A et al [13]. Similarly in our study, the perivascular spread was seen predominantly involving cavernous sinuses in the form of thrombophlebitis and ICA in the form of vasculitis, thrombosis, and mycotic aneurysms.

Recurrence of ROCM after FESS or surgical debridement was most common in the extraconal fat of orbit. The other sites for recurrence were retro-antral, pterygopalatine fossa, pre-maxillary intra-cranial regions, and palate. Cha Dong Yeo et al. also found that post-FESS recurrence of ROCM can occur and cause persistence or recurrence of symptoms [14]. No large-scale data is available regarding the recurrence of ROCM after FESS.

## CONCLUSION:

Based on our study, Diabetes mellitus and steroid treatment were common comorbidities associated in rhino-orbital-cerebral mucormycosis in patients with history of COVID-19. Peri-neural and peri vascular spread were equally common pathway of spread of infection as compared to direct spread.

The common areas of recurrent infection in patients who had undergone FESS were orbital, retro-maxillary, palate and intra-cranial in descending order.Orbital and retro-maxillary extension were most common locations of spread of the infection in conservatively managed patients.

Thus MRI is an exemplary modality for evaluation of extension of ROCM as it allows assessment of soft tissues, neural and vascular involvement, detection of intracranial complications. CT plays complimentary role for evaluation of bony structures.

## REFERENCES


1. Garg D, Muthu V, Sehgal IS, Ramachandran R, Kaur H, Bhalla A, Puri GD, Chakrabarti A, Agarwal R. Coronavirus Disease (Covid-19) Associated Mucormycosis (CAM): Case Report and Systematic Review of Literature. Mycopathologia. 2021 May;186(2):289-298. DOI: 10.1007/s11046-021-00528-2. Epub 2021 Feb 5. PMID: 33544266; PMCID: PMC7862973.
2. Jeong W, Keighley C, Wolfe R, et al.: The epidemiology and clinical manifestations of mucormycosis: a systematic review and meta-analysis of case reports. ClinMicrobiol Infect. 2019, 25:26-34. 10.1016/j.cmi.2018.07.011. Epub 2018 Jul 21.
3. Ismaiel WF, Abdelazim MH, Eldsoky I, et al.: The impact of COVID-19 outbreak on the incidence of acute invasive fungal rhinosinusitis. Am J Otolaryngol. 2021, 14:103080. 10.1016/j.amjoto.2021.103080. Epub ahead of print.
4. Watkinson JC, Clarke RW. Scott-Brown's otorhinolaryngology and head and neck surgery (8th Edition): Volume 1: Basic sciences, endocrine surgery, rhinology. CRCPress; Boca Raton, FL, USA: 2018. ISBN 9781138094611.
5. Joshi AR, Muthe MM, Patankar SH, Athawale A, Achhapalia Y. CT and MRI Findings of Invasive Mucormycosis in the Setting of COVID-19: Experience From A Single Center in India. AJR Am J Roentgenol. 2021 Jun 23. DOI: 10.2214/AJR.21.26205. Epub ahead of print. PMID: 34161127.
6. Hosseini SM, Borghei P: Rhinocerebral mucormycosis: pathways of spread. Eur Arch Otorhinolaryngol. 2005, 262(11):932-8. 10.1007/s00405-005-0919-0
7. Ma J, Jia R, Li J, et al. Retrospective Clinical Study of Eighty-One Cases of Intracranial Mucormycosis. J Glob Infect Dis. 2015;7(4):143-150. DOI:10. 4103/0974-777X.170497.
8. Safder S, Carpenter JS, Roberts TD, Bailey N. The "Black Turbinate" sign: An early MR imaging finding of nasal mucormycosis. AJNR Am J Neuroradiol. 2010 Apr;31(4):771-4. DOI: 10.3174/ajnr.A1808. Epub 2009 Nov 26. PMID: 19942703; PMCID: PMC7964235.
9. Sravani T, Uppin SG, Uppin MS, Sundaram C. Rhinocerebralmucormycosis: Pathology revisited with emphasis onperineural spread. Neurol India 2014;62:383-6.DOI: 10.4103/0028-3886.141252.
10. Margo CE, Linden C, Strickland-Marmol LB, Denietolis AL, McCaffrey JC, Kirk N. Rhinocerebralmucormycosis with perineural spread. Ophthalmic PlastReconstr Surg. 2007 Jul-Aug;23(4):326-7. DOI: 10.1097/IOP. 0b013e318070855b. PMID: 17667114.
11. Parsi K, Itgampalli RK, Vittal R, Kumar A. Perineural spread ofrhino-orbitalcerebralmucormycosis caused by *Apophysomyceselegans*. Ann Indian AcadNeurol2013; 16:414-7.DOI: 10.4103/0972-2327.11692.
12. Orguc S, Yücetürk AV, Demir MA, et al.: Rhinocerebral mucormycosis: perineural spread via the trigeminal nerve. J Clin Neurosci. 2005, 12(4):484-6. 10.1016/j.jocn.2004.07.015
13. Dusart A, Duprez T, Van Snick S, Godfraind C, Sindic C. Fatal rhinocerebralmucormycosis with intracavernous carotid aneurysm and thrombosis: a late complication of transsphenoidal surgery? ActaNeurol Belg. 2013 Jun;113(2):179-84. DOI: 10.1007/s13760-012-0151-9. Epub 2012 Nov 8. PMID: 23135781.
14. Cha Dong Yeo, Jong Seung Kim, Sam Hyun Kwon, Eun Jung Lee, Min Hee Lee, SuGeun Kim , YeonSeok You, June Sun Kim, Jong Hwan Lee, Ji SeobRyu.Rhinocerebralmucormycosis after functional endoscopic sinus surgery: A case report, PMID: **30572431** PMCID: PMC6319933 DOI: 10.1097/MD.0000000000013290